Effect of ECAP and ultrasonic treatment on the corrosion resistance of magnesium and its medical applications

Denis Aksenov[1,*], *Airat* Nazarov[2], *Leila* Khadzhieva[3]

[1]Institute of Molecule and Crystal Physics UFRC RAS, 450075 Ufa, Russia
[2]Institute for Metals Superplasticity Problems RAS, 450001 Ufa, Russia
[3]Kadyrov Chechen State University, Grozny, Russia

Abstract. Magnesium and its alloys are promising materials for manufacturing bioresorbable implants. Various combinations of thermo-mechanical processing are used to improve the mechanical properties and corrosion resistance of magnesium alloys, forming the necessary structural state, which, in turn, requires determining the influence of various structural factors (grains, grain boundaries, dislocations, second-phase particles, etc.) on the complex properties of 'strength - corrosion resistance'. In this study, an experiment was conducted to determine the influence of structural changes in pure magnesium on mechanical properties and corrosion resistance in a physiological environment after deformation using equal channel angular pressing (ECAP) and post-deformation ultrasonic treatment. It was found that ECAP and subsequent ultrasonic treatment lead to a twofold increase in the yield strength of magnesium from 30 to 60 MPa. The increase in microhardness after ECAP is 50 MPa, while ultrasonic treatment results in an increase in microhardness by 230 MPa. After deformation, corrosion resistance changes significantly: ECAP reduces the corrosion rate compared to the initial state of magnesium by approximately 7 times, to values of 7 mm/year. Subsequent volume ultrasonic treatment does not lead to significant changes in the corrosion rate, which in this case was 10 mm/year.

1 Introduction

Magnesium possesses high specific strength, low density, and a Young's modulus closest among metals and alloys to that of human bone. Additionally, magnesium, as a trace element, is necessary for the normal functioning of the human body. All of these characteristics make it one of the most promising materials for manufacturing bioresorbable implants. However, pure magnesium is characterized by rapid corrosion in physiological environments and, due to gradual dissolution, insufficient strength, necessitating the improvement of its corrosion and mechanical properties. Alloying magnesium with elements such as zinc, zirconium [1-4], calcium [5,6], or rare earth elements [7,8], allows for an increase in magnesium's

* Corresponding author: AksyonovDA@mail.ru

© The Authors, published by EDP Sciences. This is an open access article distributed under the terms of the Creative Commons Attribution License 4.0 (https://creativecommons.org/licenses/by/4.0/).

corrosion resistance. However, deformation processing aimed at strengthening can ambiguously affect the corrosion resistance of these materials.

In addition to structural elements inherent in polycrystals of pure metals, such as grain boundaries, point and line defects, grains, in alloys, the corrosion resistance will also be influenced by second-phase particles [9,10] and solid solution concentration [11]. It is also important to consider the synergistic effect of these factors on corrosion resistance.

According to research dedicated to magnesium alloys [12], grain refinement in some cases can lead to improved corrosion resistance due to the formation of an oxide film and its fixation along the boundaries, including twin boundaries [13,14]. However, increasing dislocation density during deformation significantly accelerates the corrosion process [15,16]. One of the effective methods to address this issue is annealing [17,18], to increase system equilibrium, but this usually leads to a decrease in material strength due to grain growth. Another important parameter influencing corrosion resistance is the type and distribution characteristics of second-phase particles. Particles containing, for example, Zn and Zr act as cathodic and accelerate the dissolution of the matrix at the interphase boundary [19].

The authors of this study proposed the use of bulk ultrasonic treatment on samples of deformed magnesium alloy to improve system equilibrium [20]. The works by [21-23] demonstrate that ultrasonic treatment does not alter grain size or dislocation density.

However, in order to determine the influence of ultrasound on the structure of magnesium alloys and the impact of structural parameters on corrosion resistance and strength characteristics, it is necessary to assess the effect of ultrasonic treatment on the structure independently of synergistic effects with particles and solid solution, i.e., conduct experiments on pure magnesium. In our previous work [24], positive results were demonstrated in terms of increased strength while maintaining corrosion resistance of the Mg-Zn-Zr alloy system subjected to deformation using ECAP. Therefore, this study investigates the influence of bulk ultrasonic treatment on the structure and corrosion resistance of pure magnesium strengthened by ECAP.

2 Materials and methods

Magnesium with a purity of 99.9% wt. was used in the work. The metal was obtained in ingot form after casting. To stabilize the structure, annealing was conducted at a temperature of 200±10 °C for 24 hours. Subsequently, cylindrical samples with a diameter of 20 mm and a length of 100 mm were cut using an electroerosion machine.

Deformation using the ECAP method with a channel intersection angle of 120° was performed at a temperature of 400±10 °C and a speed of 1 mm/s. One deformation cycle was conducted with an accumulated strain of approximately e~0.7.

Post-deformation bulk ultrasonic treatment was carried out according to the scheme shown in Fig. 1. An ultrasonic transducer (2), powered by a generator (1), excites alternating compression-tension stresses in a half-wave cylindrical waveguide (3), the antinode of which is located in the middle of the sample (4) fixed in it. Sample forms a common oscillatory system with the waveguide, since it is tightly clamped using a pressure cylinder with a threaded connection (5). The amplitude of ultrasonic vibrations of waveguide end was 10 μm, and the treatment duration was 120 seconds.

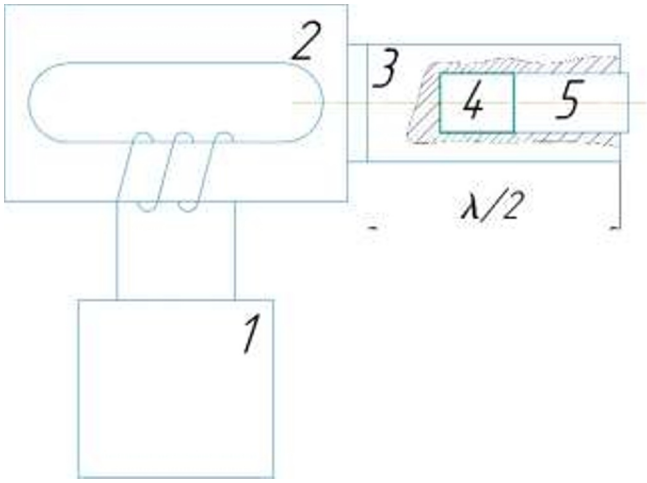

Fig. 1. Schematic diagram of ultrasonic treatment: 1 — ultrasonic generator; 2 — transducer; 3 — waveguide; 4 — sample; 5 — pressure cylinder

The investigation of the structure in longitudinal section was conducted using an Olympus GX51 optical microscope.

X-ray structural analysis was performed on a Bruker D8 Advance diffractometer using CuKα radiation, with continuous sample rotation (20 degrees/min), and step scanning (step 0.02°, exposure 1 s) in the angular range of $2\Theta = 30°–90°$. An approach based on modified Williamson-Hall and Warren-Averbach methods and proposed in works [25, 26] was implemented to estimate dislocation density.

Mechanical testing was carried out according to GOST 1497-84 standards. For tensile tests, we used proportional cylindrical samples with a working part diameter of 3 mm and an initial calculated length of 15 mm, the axes of which were directed along the deformation axis. Tensile tests were performed on an electromechanical testing system Instron 5982 for static tests at room temperature, at a speed of 1 mm/min.

Immersion corrosion tests were conducted according to ASTM G31 standard. The mass of samples was measured using analytical balances GR-200 (A&D, Japan) with an accuracy of 0.1 mg. Samples were immersed in 50 ml of Ringer's solution (0.86% NaCl, 0.03% KCl, 0.033% $CaCl_2$, pH 7.4) and kept at a temperature of 36±1 °C. Prior to mass measurement, corrosion products ($Mg(OH)_2$) were removed from the samples. Rinse, as per ASTM G1 standard for corrosion product removal, was carried out in a wash solution consisting of 200 g CrO_3, 10 g $AgNO_3$, 20 g $Ba(NO_3)_2$, and 1000 ml H_2O in an ultrasonic bath. Weighing was done afterward. The solution was replaced daily for the first 5 days, then every 5 days thereafter. Corrosion rate (mm/year) was calculated using the formula specified in ASTM G31:

$$\text{Corrosion Rate} = (K \cdot W)/(A \cdot T \cdot D) \quad (1)$$

where: K - a constant ($8.76 \cdot 10^4$), T - time of exposure in hours, A - area in cm^2, W - mass loss in grams, and D - density in g/cm^3.

3 Results and discussions

In its initial annealed state (24 hours at 200±10°C), pure magnesium has a coarse-grained structure (see Figure 2). The average grain size is 490±170 μm. Some grains exhibit twin

boundaries. After ECAP, grains elongate along the shear direction. Along the boundaries of large deformed grains with sizes of 350±120 μm, small recrystallized grains with sizes of 10-20 μm are observed. Thus, dynamic recrystallization occurs during ECAP at a temperature of 400±10°C. Additionally, some grains exhibit twins up to 10 μm wide. After bulk ultrasonic treatment, the structure's appearance remains largely unchanged. Large deformed grains with recrystallized grains sized 10-20 μm, primarily located along their boundaries, are observed.

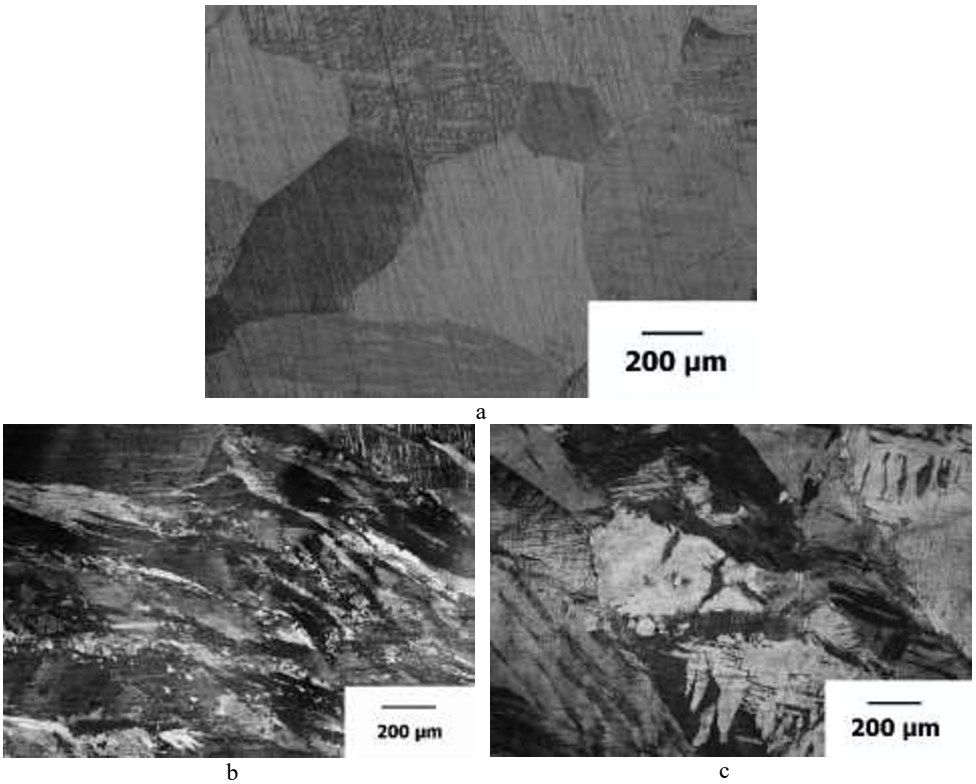

a

b c

Fig. 2. The structure of the initial magnesium (a), after ECAP, 1 cycle (b), and post-deformation ultrasonic treatment (c)

X-ray structural analysis indicates a refinement of the structure during ECAP (see Table 1). It was found that the average grain size decreases from 300 to 142 nm. Microstrain in the lattice increases almost twofold, and dislocation density increases approximately by 2.5 times, reaching a value of $7.9 \cdot 10^{14}$ m^{-2}. Subsequent volumetric ultrasonic treatment does not lead to significant changes in these characteristics: the values of CSR, microstrain and dislocation density remain approximately at the same level.

Table 1. X-ray diffraction analysis results.

State	Lattice parameter, nm		CSR, nm	Microstrain	Dislocation density, 10^{14} m^{-2}
	a	c			
Initial	0.3209	0.5210	300±27	0.1197±0.0013	2.9
ECAP 1p. 400 °C	0.3209	0.5210	142±23	0.1909±0.038	7.9
ECAP 1p. 400 °C +US	0.3209	0.5215	166±25	0.2011±0.0017	8.0

Table 2 presents the results of mechanical tests of samples. Analysis of the obtained data shows that deformation at high temperature does not lead to an increase in the material's

ultimate strength. However, the yield strength increases both after ECAP and after post-deformation bulk ultrasonic treatment. Additionally, there is an increase in microhardness. ECAP results in a microhardness increase of 50 MPa compared to the initial state, while the increase due to bulk ultrasonic treatment is 230 MPa. It should be noted here that despite the fact that the yield strength of magnesium after ECAP and ultrasonic treatment did not change so significantly, microhardness, which is a characteristic of the surface, does not satisfy the often-found relationship with the yield strength, expressed as $HV = 3 \cdot \sigma_{0.2}$. [27, 28].

Table 2. Mechanical properties.

State	UTS, MPa	YTS, MPA	Elongation, %	HV, MPa
Initial	120±5	30±3	6±1	370±30
ECAP 1p. 400 °C	125±5	45±3	7±1	420±30
ECAP 1p. 400 °C+US	115±5	60±3	7±1	650±40

Immersion corrosion studies in Ringer's solution showed high corrosion resistance of samples after ECAP and ECAP+US treatment (see Figure 3). Samples in the initial state dissolved within 5 days at a minimum corrosion rate of 49 mm/year. ECAP leads to the formation of a structural state that ensures dissolution at a rate 7 times slower than the initial state. Post-deformation ultrasonic treatment results in a slight increase in corrosion rate, from ~7 to ~10 mm/year. These findings are crucial regarding magnesium matrix, as they indicate that grain refinement and increased dislocation density, while maintaining these characteristics after bulk ultrasonic treatment, do not lead to increased corrosion rates. In studies related to the corrosion resistance of magnesium alloys, more attention should be given to factors such as solid solution concentration, presence of second phase particles, their sizes, and distribution.

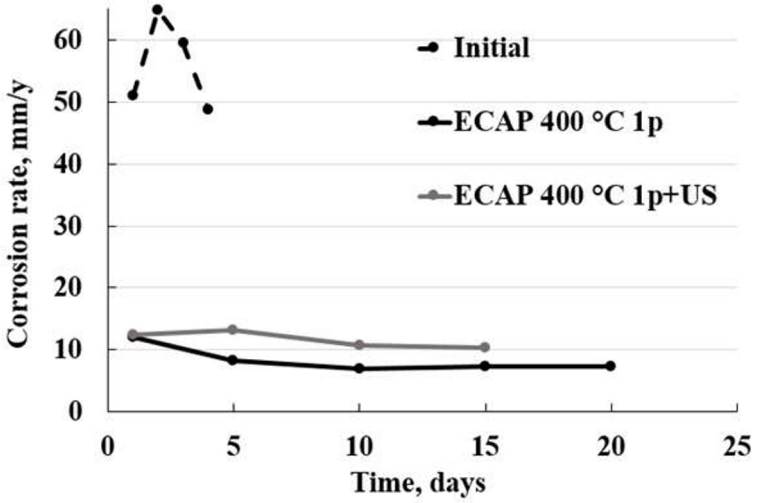

Fig. 3. The corrosion rate of magnesium samples in Ringer's solution.

The image of the surface of pure magnesium after corrosion exposure in Ringer's solution for 1 day for conditions after ECAP and post-deformation ultrasonic treatment is presented in Figure 4. Analysis of the images shows that the predominant type of corrosion is transgranular corrosion. In addition to this, uniform corrosion is observed within some grains in both conditions.

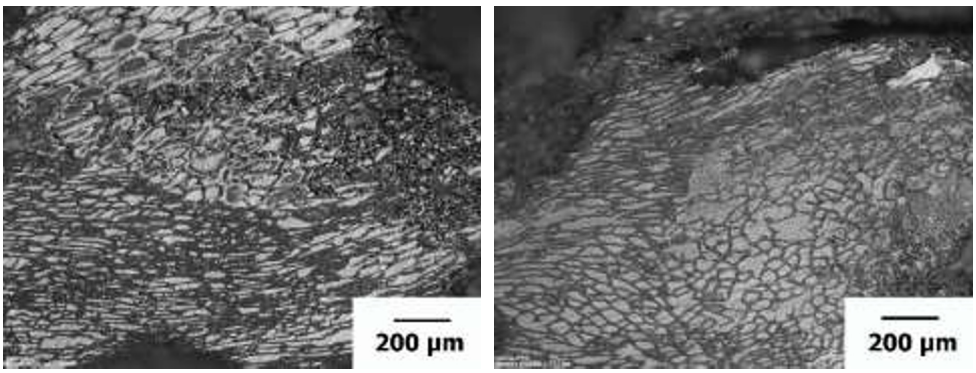

a b

Fig. 4. Surface images of pure magnesium samples after ECAP (a) and ECAP with ultrasonic treatment (b)

4 Conclusions

ECAP of pure magnesium with an accumulated strain level of e~0.7 at a temperature of 400±10 °C and a deformation rate of 1 mm/s leads to structure refinement through the transformation of initial coarse grains to sizes about 350 μm and the formation of new fine recrystallized grains sized 10-20 μm. The dislocation density nearly doubles during this process. Subsequent post-deformation bulk ultrasonic treatment does not result in an increase or decrease in dislocation density or grain size.

During ECAP of pure magnesium, there is an increase in the average microhardness and yield strength by 50 MPa (13%) and 15 MPa (50%), respectively. Subsequent post-deformation bulk ultrasonic treatment in the deformed state leads to further increases in microhardness by 55% to 650 MPa and yield strength by 30% to 60 MPa.

ECAP of pure magnesium under the proposed conditions leads to a decrease in corrosion rate in a physiological environment by approximately 7 times. With an initial corrosion rate of 49 mm/year, the corrosion rate of the sample after ECAP decreases to 7 mm/year. Subsequent post-deformation bulk ultrasonic treatment increases the corrosion rate to 10 mm/year.

The work was supported by the Russian Science Foundation (project No. 22-79-10325).

References

1. C. Bettles, M. Gibson, Jom **57**, 5 (2005)
2. C. Zhang, S. Guan, L. Wang, S. Zhu, L. Chang, Journal of Materials Research **32**, 6 (2017)
3. Y. Ding, C. Wen, P. Hodgson, Y. Li, Journal of materials chemistry B **2**, 14 (2014)
4. P. Jiang, C. Blawert, M. L. Zheludkevich, Corrosion and Materials Degradation **1**, 1 (2020)
5. R. Radha, D. Sreekanth, Journal of magnesium and alloys **5**, 3 (2017)
6. R. C. Zeng, W. C. Qi, H. Z. Cui, F. Zhang, S. Q. Li, E. H. Han, Corrosion Science **96** (2015)
7. C. Guo, L. Liu, H. Liu, F. Qian, Y. Zhou, L. Wang, J. Wang, Journal of Alloys and Compounds **985** (2024)

8. Y. Zhang, Y. Liu, R. Zheng, Y. Zheng, L. Chen, Journal of Rare Earths (2023)
9. C. Y. Hsieh, S. Y. Huang, Y. R. Chu, H. W. Yen, H. C. Lin, D. S. Shih, Y. L. Lee, Journal of Materials Research and Technology **22** (2023)
10. J. Wang, Y. Yuan, T. Chen, L. Wu, X. Chen, B. Jiang, F. Pan, Journal of Magnesium and Alloys **10**, 7 (2022)
11. H. S. Sidhu, B. Singh, P. Kumar, Materials Today: Proceedings **46** (2021)
12. D. L. Merson, A. I. Brilevsky, P. N. Myagkikh, M. V. Markushev, A. Vinogradov, Letters on Materials **10**, 2 (2020)
13. C. Yan, Y. Xin, X. B. Chen, D. Xu, P. K. Chu, C. Liu, Q. Liu, Nature communications **12**, 1 (2021)
14. Z. Xia, R. Huang, C. Yan, Y. Xin, B. Feng, J. Xu, L. Zhao, Journal of Materials Research and Technology **29** (2024)
15. H. Y. Choi, W. J. Kim, Journal of the Mechanical Behavior of Biomedical Materials **51** (2015)
16. H. Wang, X. Xiao, C. Qiao, D. Wu, Y. Wang, Z. Liu, L. Hao, Materials Letters **355** (2024)
17. X. Cui, Y. Yang, Y. Zhu, M. Li, C. Wen, B. Jiang, F. Pan, Journal of Materials Research and Technology **22** (2023)
18. K. K. Verma, S. Kumar, S. Suwas, Materials Science and Engineering: A **821** (2021)
19. E. V. Parfenov, O. B. Kulyasova, V. R. Mukaeva, B. Mingo, R. G. Farrakhov, Y. V. Cherneikina, R. Z. Valiev, Corrosion Science **163** (2020)
20. D. A. Aksenov, A. A. Nazarov, G. I. Raab, A. G. Raab, E. I. Fakhretdinova, R. N. Asfandiyarov, M. A. Shishkunova, Y. R. Sementeeva, Materials **15**, 20 (2022)
21. A. A. Nazarova, R. R. Mulyukov, V. V. Rubanik, Y. V. Tsarenko, A. A. Nazarov, The Physics of Metals and Metallography **110** (2010)
22. A. Samigullina, A. A. Nazarov, R. R. Mulyukov, Y. V. Tsarenko, V. V. Rubanik, Reviews on advanced materials science **39**, 1 (2014)
23. A. P. Zhilyaev, A. A. Samigullina, A. E. Medvedeva, S. N. Sergeev, J. M. Cabrera, A. A. Nazarov, Materials Science and Engineering: A **698** (2017)
24. D. A. Aksenov, E. I. Fakhretdinova, R. N. Asfandiyarov, A. G. Raab, A. E. Sharipov, M. A. Shishkunova, Y. R. Sementeeva, Frontier Materials & Technologies **1** (2024)
25. T. Ungar, A. Borbely, Applied Physics Letters **69** (1996)
26. A. Muiruri, M. Maringa, W. Preez, Materials **13** (2020)
27. P. Zhang, S. X. Li, Z. F. Zhang, Materials Science and Engineering A **529** (2011)
28. C. H. C´aceres et al., Materials Science and Engineering A **402** (2005)